Journal of
Mechanics of
Materials and Structures

ENERGY BASED FRACTURE IDENTIFICATION IN MASONRY STRUCTURES: THE CASE STUDY OF THE CHURCH OF "PIETÀ DEI TURCHINI"

Antonino Iannuzzo

Volume 14, No. 5 December 2019

msp

JOURNAL OF MECHANICS OF MATERIALS AND STRUCTURES
Vol. 14, No. 5, 2019
dx.doi.org/10.2140/jomms.2019.14.683

msp

ENERGY BASED FRACTURE IDENTIFICATION IN MASONRY STRUCTURES: THE CASE STUDY OF THE CHURCH OF "PIETÀ DEI TURCHINI"

ANTONINO IANNUZZO

The present work deals with the identification of fractures in "old" masonry structures modelled by extending the Heyman model to continua, particularly to 2D structures composed of normal rigid no-tension material, and subjected to given loads and settlements. The equilibrium problem is formulated as an energy minimum search and two numerical methods for approximating the solution are adopted, namely the PRD method and the C^0 method. By using the PRD method, the energy is minimized within the set of piecewise rigid displacements (PRD), whilst with the second one, the search of the minimum is restricted to continuous (C^0) displacement fields. A case study, regarding the church of "Pietà dei Turchini" (an XVII century church located in Naples), is here presented to illustrate how an admissible class of kinematical data (i.e., foundation displacements) associated to a given crack pattern can be identified by using an iterative procedure. Firstly, the analysis is conducted through the PRD method and secondly, the C^0 method is used to assess the quality of the first solution, and to make comparisons between these two approaches showing pro and contra of both methods.

1. Introduction

The first to propose the application of limit analysis (LA) to voussoir arches was Kooharian [1952]. Some years later, Heyman [1966] laid a theoretical basis for the application of LA to generic masonry structures through the clear and rigorous formulation of three basic material restrictions: (i) masonry has no tensile strength, (ii) masonry has infinite compressive strength, (iii) sliding does not occur.

In his work, Heyman studied in deep the arch and extended the analysis to a wide range of masonry structures, with particular reference to Gothic cathedrals and their peculiar structural elements.

The three assumptions of Heyman, on one hand, constitute the necessary ingredients for the application of the two basic theorems of LA to masonry structures (see [Heyman 1998; Huerta 2006; 2008; Kurrer 2008]), and on the other hand give also a mathematical base to the equilibrium approach taken from the study of Hooke [1676] and Gregory [1695] and used by many scientists in the past centuries, such as Couplet [1729; 1730], Danyzy [1732/1778], Poleni [1748], Le Seur et al. [1742], Coulomb [1776], Barlow and Yvon de Villarceau [Yvon Villarceau 1853; 1854].

The present paper deals with the application of Heyman's theory to a real masonry structure, and in particular, is concerned with the identification of the cracks appearing in the walls of the church of "Pietà dei Turchini" in Naples. The material composing the structure is modelled as normal rigid no-tension (NRNT). The NRNT material is rigid in compression, but extensional deformations, regular or singular, are allowed at zero energy price.

Keywords: masonry, unilateral materials, settlements, piecewise rigid displacements, continuous displacements, concentrated and smeared cracks.

For discussion and applications of limit analysis to masonry-like structures the reader can refer to [Livesley 1978; Castellano 1988; Como 1992; Di Pasquale 1984; Giuffrè 1991; Angelillo 1993; 2014; 2019; Bagi 2014; Block et al. 2006; Block and Lachauer 2013; 2014; Block 2009; Del Piero 1998; Ochsendorf 2006; Sacco 2014; Angelillo et al. 2014; 2018; Brandonisio et al. 2015; 2017; Cennamo et al. 2018; Gesualdo et al. 2017; Fortunato et al. 2018; Fraddosio et al. 2019; Marmo and Rosati 2017; Marmo et al. 2018; Shin et al. 2016; Portioli et al. 2014; Romano and Romano 1979; Van Mele et al. 2012; Zuccaro et al. 2017].

Since in NRNT structures extensional deformation could appear as either diffuse (smeared cracks) or concentrated (macroscopic cracks), and there is any reason to prefer one type of fractures upon the others, on an energy ground, the crack pattern of the church is identified on adopting two different numerical strategies, namely the PRD and C^0 methods (for more examples the reader can refer to [Iannuzzo 2017; Iannuzzo et al. 2018b; 2018c]). With both methods, the solution of the boundary value problem (BVP) is searched by adopting a displacement approach, and by restricting to small displacement fields, it reduces to the search of the minimum of a linear functional, namely the total potential energy (TPE). With the PRD method, the search of the solution of the BVP is performed within the set of piecewise rigid displacements: the strain admits only a singular part, represented by line Dirac deltas, and it is concentrated along the skeleton of the mesh, that is along the element interfaces; the C^0 method, instead, approximates the solution within the set of continuous displacements and then the strain admits only a regular part. The two methods represent two different numerical strategies to implement numerically Heyman's material restrictions to continua.

2. Material restrictions, BVP and the energy criterion for NRNT materials

NRNT materials. The Heyman's constraints ((i), (ii), (iii)) can be extended to 2D continua on introducing suitable unilateral material restrictions on stress and strain. A 2D masonry structure is modelled as a continuum occupying the region Ω of the Euclidean space $\mathbb{R}^2$. Restricting to small strain and displacement fields, we denote $\boldsymbol{T}$ the stress inside Ω, $\boldsymbol{u}$ the displacement of material points $\boldsymbol{x}$ belonging to Ω and $\boldsymbol{E}$ the infinitesimal strain adopted as the strain measure.

The so-called normal rigid no-tension (NRNT) material is defined by the following three restrictions:

$$\boldsymbol{T} \in \mathrm{Sym}^-, \quad \boldsymbol{E} \in \mathrm{Sym}^+, \quad \boldsymbol{T} \cdot \boldsymbol{E} = 0, \tag{1}$$

where Sym^-, Sym^+ are the mutually polar cones (see Figure 1) of negative and positive semidefinite symmetric tensors.

The restrictions (1) are equivalent to the so-called *normality conditions*:

$$\boldsymbol{T} \in \mathrm{Sym}^-, \quad (\boldsymbol{T} - \boldsymbol{T}^*) \cdot \boldsymbol{E} \geq 0, \quad \forall \boldsymbol{T}^* \in \mathrm{Sym}^-, \tag{2}$$

and to the *dual normality conditions*:

$$\boldsymbol{E} \in \mathrm{Sym}^+, \quad (\boldsymbol{E} - \boldsymbol{E}^*) \cdot \boldsymbol{T} \geq 0, \quad \forall \boldsymbol{E}^* \in \mathrm{Sym}^+. \tag{3}$$

The restrictions defining the NRNT material are then the essential ingredients for the application of the theorems of LA (see [Kooharian 1952; Giaquinta and Giusti 1985; Livesley 1978; Fortunato et al. 2014; 2016; Milani 2011; Angelillo et al. 2010; Addessi and Sacco 2018]).

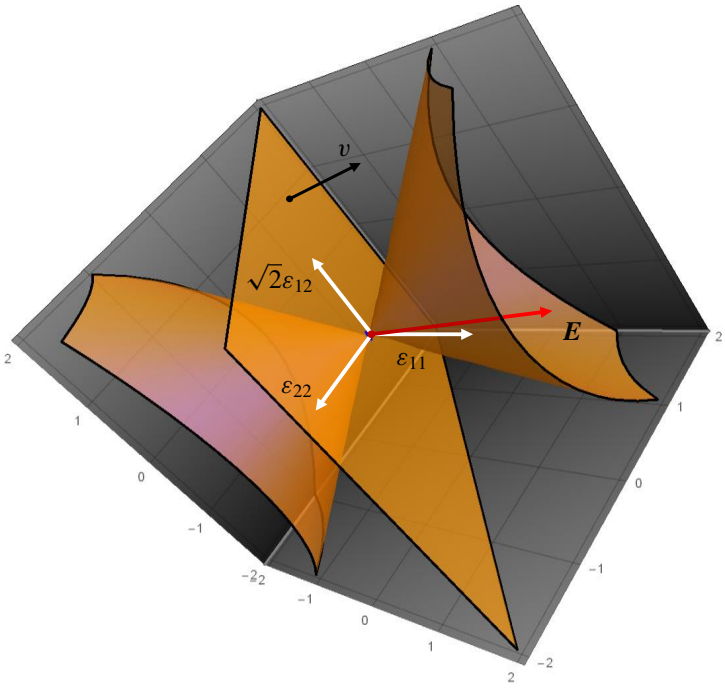

Figure 1. A three-dimensional geometrical representation of relation $(1)^2$ in the space $(\varepsilon_{11}, \varepsilon_{22}, \sqrt{2}\,\varepsilon_{12})$: the cone $C : \det \boldsymbol{E} \geq 0$ and the plane $\pi : \mathrm{tr}\boldsymbol{E} = 0$. A generic tensor $\boldsymbol{E} \in \mathrm{Sym}^+$ is represented. For the symbols adopted the reader can refer to (31) and (32), and to the subsequent paragraph.

The boundary value problem. The equilibrium of a 2D masonry structure, modelled as a continuum composed of NRNT material and subject to given loads and settlements, can be formulated as a Boundary Value Problem (BVP) in the following form: *"find a displacement field* $\boldsymbol{u}$ *and the corresponding strain* $\boldsymbol{E}$*, and a stress field* $\boldsymbol{T}$ *such that*

$$\boldsymbol{E} = \tfrac{1}{2}(\nabla \boldsymbol{u} + \nabla \boldsymbol{u}^T), \quad \boldsymbol{E} \in \mathrm{Sym}^+, \quad \boldsymbol{u} = \bar{\boldsymbol{u}} \text{ on } \partial\Omega_{\mathrm{D}}, \tag{4}$$

$$\mathrm{div}\boldsymbol{T} + \boldsymbol{b} = 0, \quad \boldsymbol{T} \in \mathrm{Sym}^-, \quad \boldsymbol{T}\boldsymbol{n} = \bar{\boldsymbol{s}} \text{ on } \partial\Omega_{\mathrm{N}}, \tag{5}$$

$$\boldsymbol{T} \cdot \boldsymbol{E} = 0, \text{"} \tag{6}$$

where $\boldsymbol{n}$ is the unit outward normal to the boundary $\partial\Omega$, $\bar{\boldsymbol{u}}$ are the boundary displacements on the constrained part $\partial\Omega_{\mathrm{D}}$ and $\bar{\boldsymbol{s}}$ are the given tractions on the loaded part $\partial\Omega_{\mathrm{N}}$ (see [Angelillo and Fortunato 2004]).

Concentrated strain and stress. For NRNT materials, it has been shown (see [Giaquinta and Giusti 1985; Šilhavý 2014]) that the strain and stress are bounded measures and can be decomposed into the sum of two parts:

$$\boldsymbol{E} = \boldsymbol{E}^r + \boldsymbol{E}^s, \quad \boldsymbol{T} = \boldsymbol{T}^r + \boldsymbol{T}^s, \tag{7}$$

where $(\cdot)^r$ is the regular part (i.e., absolutely continuous with respect to the area measure) and $(\cdot)^s$ is the singular part.

A nonzero singular part of the strain or of the stress corresponds to the possibility of admitting discontinuities of the displacement vector or of the stress vector across certain curves. For a more detailed review about jump discontinuities of stress or of displacement for masonry-like material, the reader can refer to [Angelillo et al. 2016].

Displacement approach. A solution of the BVP through the *displacement approach* consists in the search of a displacement field $\boldsymbol{u} \in \mathcal{K}$ for which there exists a stress field $\boldsymbol{T} \in \mathcal{H}$ such that $\boldsymbol{T} \cdot \boldsymbol{E}(u) = 0$, where $\mathcal{K}$ and $\mathcal{H}$ are the sets of kinematically admissible displacements and statically admissible stresses, defined as

$$\mathcal{K} = \{\boldsymbol{u} \in S / \boldsymbol{E} = \tfrac{1}{2}(\nabla \boldsymbol{u} + \nabla \boldsymbol{u}^T) \in \mathrm{Sym}^+ \quad \text{and} \quad \boldsymbol{u} = \bar{\boldsymbol{u}} \text{ on } \partial\Omega_{\mathrm{D}}\}, \tag{8}$$

$$\mathcal{H} = \{\boldsymbol{T} \in S' / \mathrm{div}\boldsymbol{T} + \boldsymbol{b} = 0, \quad \boldsymbol{T} \in \mathrm{Sym}^-, \quad \boldsymbol{T}\boldsymbol{n} = \bar{\boldsymbol{s}} \text{ on } \partial\Omega_{\mathrm{N}}\}, \tag{9}$$

where S, S' are two suitable functional spaces (see [Angelillo and Rosso 1995; Chambolle et al. 2007]). It is worth noting that, by adopting a displacement approach, the functional space S defines the set where the solution has to be found: in particular, as shown in what follows, the two numerical approximations, namely PRD and C^0 methods, work on two different subsets of the starting set $\mathcal{S}$.

Energy criterion. The energy $\mathcal{P}(\boldsymbol{u})$ for brittle materials is the sum of the potential energy of the applied loads and of the elastic and interface ones, with this latter necessary to activate a crack system on a set of internal surfaces (see [Gesualdo et al. 2018; Monaco et al. 2014; Angelillo et al. 2012; Gesualdo and Monaco 2015]). For Heyman's material the total potential energy is just the potential energy of the external loads [De Serio et al. 2018], namely

$$\mathcal{P}(\boldsymbol{u}) = -\int_{\partial\Omega_{\mathrm{N}}} \bar{\boldsymbol{s}} \cdot \boldsymbol{u} \, \mathrm{d}s - \int_{\Omega} \boldsymbol{b} \cdot \boldsymbol{u} \, \mathrm{d}a. \tag{10}$$

The search of a solution of the BVP through a displacement approach could be got by looking for the minimizer $\boldsymbol{u}^\circ$ of $\mathcal{P}(\boldsymbol{u})$ as in [Iannuzzo 2017], namely

$$\mathcal{P}(\boldsymbol{u}^\circ) = \min_{\boldsymbol{u} \in \mathcal{K}} \mathcal{P}(\boldsymbol{u}) \quad \text{with } \boldsymbol{u} \in \mathcal{K}. \tag{11}$$

It is worth noticing that the existence of a minimizer $\boldsymbol{u}^\circ$ guarantees also the equilibrium of the loads imposed on the structure.

3. The search for an approximate solution in two different subsets of $\mathcal{K}$: PR and C^0 methods

In this section, two possible approximations of the solution of the BVP, are introduced, namely the PRD method and the C^0 method. These approximations are obtained by restricting the search of the minimizer to two suitable subsets of the set $\mathcal{K}$. With the PRD method, the energy is minimized in the set $\mathcal{S}_{\mathrm{PRD}} \subset \mathcal{S}$ of piecewise rigid displacements, whilst with the C^0 method the search of the minimum is restricted to the space of continuous displacements $\mathrm{C}^0 \subset \mathcal{S}$.

3.1. ***PRD method.*** The first approximated solution of problem (11) is obtained by restricting the search of the minimum to the subset $\mathcal{S}_{\mathrm{PRD}} \subset \mathcal{S}$ of piecewise rigid displacements, and then the set of kinematically admissible displacements becomes

$$\mathcal{K}_{\mathrm{PRD}} = \{\boldsymbol{u} \in \mathcal{S}_{\mathrm{PRD}} / \boldsymbol{E} \in \mathrm{Sym}^{+} \quad \text{and} \quad \boldsymbol{u} = \bar{\boldsymbol{u}} \text{ on } \partial\Omega_{\mathrm{D}}\} \subset \mathcal{K}, \tag{12}$$

where $\mathcal{K}_{\mathrm{PRD}}$ is an infinite-dimensional space and can be discretized by considering a proper finite subset, namely $\mathcal{K}^{M}_{\mathrm{PRD}}$, generated by a finite polygonal partition of the whole domain Ω:

$$(\Omega_i)_{i\in\{1,2,\ldots,M\}}. \tag{13}$$

The minimizer $\boldsymbol{u}^{0}_{\mathrm{PRD}} \in \mathcal{K}^{M}_{\mathrm{PRD}}$ of the total potential energy, namely

$$\mathcal{P}(\boldsymbol{u}^{0}_{\mathrm{PRD}}) = \min_{\boldsymbol{u}\in\mathcal{K}^{M}_{\mathrm{PRD}}} \mathcal{P}(\boldsymbol{u}), \tag{14}$$

constitutes an approximation of the solution $\boldsymbol{u}^{0}$ of the exact problem (11), in the subset $\mathcal{K}^{M}_{\mathrm{PRD}}$ and, in this sense, represents the approximate solution of the BVP obtained by using the PRD method. The numerical way used to solve the discretized problem (14) under NRNT restrictions is briefly described in what follows.

The boundary $\partial\Omega_i$ of the generic (convex) polygon Ω_i is composed of straight segments (from here on called *interfaces*) of length ℓ and whose extremities are denoted generically 0 and 1. Each segment is associated with a unit normal $\boldsymbol{n}$ and a tangent vector $\boldsymbol{t}$. Since the number of elements of the partition (13) is M, a generic piecewise rigid displacement $\boldsymbol{u} \in \mathcal{K}^{M}_{\mathrm{PRD}}$ can be expressed through a vector $\boldsymbol{U}$ of $3M$ components representing the $3M$ rigid body parameters of translation and rotation of each element. Then, the set $\mathcal{K}^{M}_{\mathrm{PRD}}$ is in one-to-one correspondence with the set $\mathbb{K}^{M}_{\mathrm{PRD}}$ generated by $\boldsymbol{U} \in \mathbb{R}^{3M}$.

For piecewise rigid displacements, the strain $\boldsymbol{E}$ coincides with its singular part $\boldsymbol{E}^{s}$ concentrated along the interfaces and can be written as

$$\boldsymbol{E} = v\,\delta(\Gamma)\,\boldsymbol{n}\otimes\boldsymbol{n} + \tfrac{1}{2}w\,\delta(\Gamma)(\boldsymbol{t}\otimes\boldsymbol{n} + \boldsymbol{n}\otimes\boldsymbol{t}), \tag{15}$$

where v, w are the normal and tangential components of the displacement jump across the interface Γ. The displacement jump is modelled through the use of the Dirac delta function $\delta(\Gamma)$ having Γ as support. Relation (15) represents the most general form of the strain tensor in the subset $\mathcal{K}^{M}_{\mathrm{PRD}}$. Nevertheless, by taking into account the normality conditions (2) or equivalently the Heyman's restrictions (1), it is deduced that on each interface among blocks a condition of unilateral contact with no sliding must be enforced, that is

$$v = [\boldsymbol{u}]\cdot\boldsymbol{n} \geq 0, \tag{16}$$

$$w = [\boldsymbol{u}]\cdot\boldsymbol{t} = 0, \tag{17}$$

where $[\boldsymbol{u}]$ represents the displacement jump on the interfaces. On allowing for internal eigenstrains along the interfaces the above conditions transform into the following nonhomogeneous relations:

$$v = [\boldsymbol{u}]\cdot\boldsymbol{n} \geq \Delta_n, \tag{18}$$

$$w = [\boldsymbol{u}]\cdot\boldsymbol{t} = \Delta_t, \tag{19}$$

Δ_n, Δ_t being given distortions. Due to conditions (16), (17) the strain must reduce to the following form:

$$\boldsymbol{E} = v\,\delta(\Gamma)\,\boldsymbol{n}\otimes\boldsymbol{n}. \tag{20}$$

By calling N the number of the interfaces, and $v(0)$, $v(1)$, $w(0)$, $w(1)$ the normal and tangential components of the relative displacements of the ends 0, 1 of any interface, restrictions [(18), (19)] are equivalent to the $2N$ inequalities

$$v(0) \geq \Delta_n^0, \quad v(1) \geq \Delta_n^1, \tag{21}$$

and to the $2N$ equalities

$$w(0) = \Delta_t, \quad w(1) = \Delta_t. \tag{22}$$

Transforming identities (22) into double inequalities, restrictions (21), (22) can be expressed in terms of $\boldsymbol{U}$. In a matrix form (see [Iannuzzo et al. 2018a]) these inequalities can be written as

$$\boldsymbol{A}\boldsymbol{U} \geq \Delta. \tag{23}$$

Finally, the minimum problem (14) which approximates the minimum problem (11) can be transformed into

$$\mathcal{P}(\boldsymbol{U}^0) = \min_{\boldsymbol{U}\in\mathbb{K}^M_{\mathrm{PRD}}} \mathcal{P}(\boldsymbol{U}), \tag{24}$$

where $\mathbb{K}^M_{\mathrm{PRD}}$ is the set

$$\mathbb{K}^M_{\mathrm{PRD}} = \{\boldsymbol{U} \in \mathbb{R}^{3M} / \boldsymbol{A}\boldsymbol{U} \geq \Delta\}. \tag{25}$$

Problem (24) is a standard linear finite-dimensional minimization problem, since the function $\mathcal{P}(\boldsymbol{U})$ is a linear function of the $3M$ vector $\boldsymbol{U}$, and all the constraints are represented by linear relations (25). It is worth noticing that problem (24) transforms the original minimization problem (11) for a continuum, into a minimization problem for a structure composed of rigid parts subject to unilateral contact conditions along the interfaces. There exist many numerical methods to obtain the solution of this minimum problem; in particular, for large problems, the solution can be searched with the interior-point algorithm (see [Mehrotra 1992; Dantzig 1963]).

3.2. C^0 *method.* A second approximation of the solution of problem (11) is obtained considering the subset C^0 (see [Iannuzzo et al. 2018c]) of $\mathcal{S}$ formed by continuous displacement fields, and then the set of kinematically admissible displacements becomes

$$\mathcal{H}_{\mathrm{C}^0} = \{\boldsymbol{u} \in \mathrm{C}^0 / \boldsymbol{E} \in \mathrm{Sym}^+ \quad \text{and} \quad \boldsymbol{u} = \bar{\boldsymbol{u}} \text{ on } \partial\Omega_{\mathrm{D}}\} \subset \mathcal{H}, \tag{26}$$

where $\mathcal{H}_{\mathrm{C}^0}$ is an infinite-dimensional space and can be discretized by considering a finite partition of the domain Ω:

$$(\Omega_i)_{i\in\{1,2,\ldots,M\}}, \tag{27}$$

where each element Ω_i is associated with a suitable Finite Element-like (FE) shape function. By calling N the total number of nodes of the FE mesh associated with the partition (27), we denote $\mathcal{H}^M_{\mathrm{C}^0}$ the subset

of $\mathcal{K}_{C^0}$ generated by this discretization. The approximated solution in $\mathcal{K}^M_{C^0}$ of the BVP obtained by applying the energy criterion, is the minimizer $\boldsymbol{u}^0_{C^0}$ of the total potential energy, namely

$$\mathcal{P}\big(\boldsymbol{u}^0_{C^0}\big) = \min_{\boldsymbol{u}\in\mathcal{K}^M_{C^0}} \mathcal{P}(\boldsymbol{u}). \tag{28}$$

The minimizer $\boldsymbol{u}^0_{C^0}$ represents the solution of the BVP with the C^0 method. The approach adopted with the C^0 method, to implement the material restrictions and to preserve the linearity of the problem, is briefly illustrated below.

Since it is assumed that FE mesh associated to the partition (27) is based on the hypothesis of continuity of the displacement fields at the nodes, the strain $(7)^1$ admits only a regular part. The NRNT material restrictions have, then, to be enforced on the strain arising inside the elements: with the C^0 method the interfaces, i.e., the boundary edges between two finite adjacent elements, play a minor role.

The displacement field $\boldsymbol{u}$ generated by the chosen FE mesh is a function of the N nodes and then is in a one to one correspondence with the nodal vector $\boldsymbol{U} \in \mathcal{R}^{2N}$ collecting the displacement components of the N nodes of the mesh. By recalling definition (1) the latent strain $\boldsymbol{E}$ has to belong to the positive semidefinite cone

$$\boldsymbol{E} \in \mathrm{Sym}^+. \tag{29}$$

This restriction, for 2D problems, is equivalent to the two following inequalities:

$$\mathrm{tr}\boldsymbol{E} \geq 0, \quad \det\boldsymbol{E} \geq 0, \tag{30}$$

and in a fixed Cartesian reference in which the strain can be represented as

$$\boldsymbol{E} = \begin{bmatrix} \varepsilon_{11} & \varepsilon_{12} \\ \varepsilon_{21} & \varepsilon_{22} \end{bmatrix}, \tag{31}$$

conditions (30) can be written in terms of Cartesian components, as

$$\varepsilon_{11}\varepsilon_{22} - \varepsilon_{12}^2 \geq 0, \quad \varepsilon_{11} + \varepsilon_{22} \geq 0, \tag{32}$$

which represent restrictions on the displacement $\boldsymbol{u}$ being $\boldsymbol{E} = \mathrm{Sym}\nabla\boldsymbol{u}$. Geometrically, the nonlinear relation $(32)^1$ defines a double cone in the space Sym whilst condition $(32)^2$ selects one of the two parts of this cone (see Figure 1). With the aim of preserving the linearity of the problem, relation $(32)^1$ is approximated through a plane envelope (see Figure 2) and then restriction $\boldsymbol{E} \in \mathrm{Sym}^+$ is enforced, in all points of the mesh, by restricting $\boldsymbol{E}$ to belong to the envelope of a finite number of tangent planes (Figure 2). Therefore, all the material restrictions are enforced by writing linear inequalities in all the nodes and can be expressed as functions of the unknown nodal displacements $\boldsymbol{U}$. Then, also in this case these inequalities can be compactly expressed in a matrix form (for more details see [Iannuzzo 2017; Iannuzzo et al. 2018c]):

$$\boldsymbol{A}\boldsymbol{U} \geq 0. \tag{33}$$

Finally, with the proposed FE approximation, the minimum problem (28) can be approximated by the following discretized minimum problem:

$$\mathcal{P}(\boldsymbol{U}^0) = \min_{\boldsymbol{U}\in\mathbb{K}^M_{C^0}} \mathcal{P}(\boldsymbol{U}), \tag{34}$$

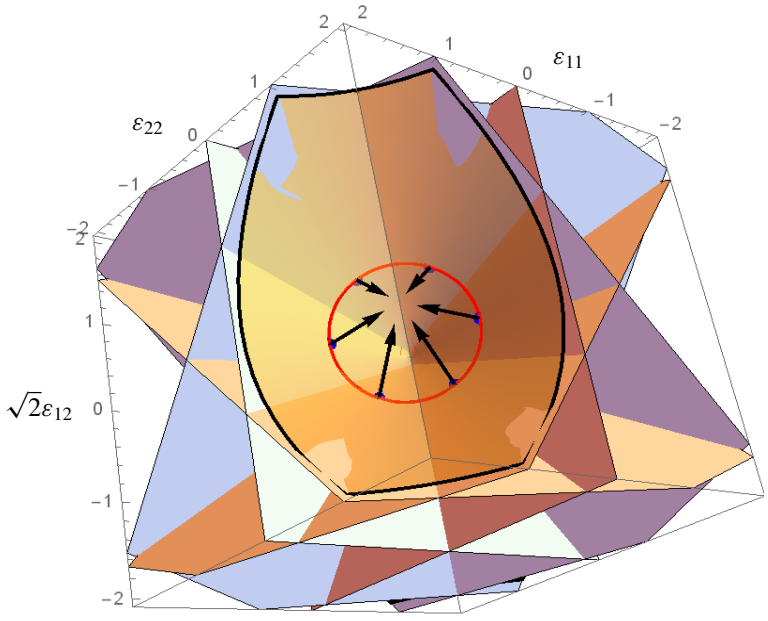

Figure 2. An envelope formed by six tangent planes and the surface gradient vectors at the tangent points are represented. The condition $\boldsymbol{E} \in \mathrm{Sym}^+$ is discretized and written as a system of inequalities by using these gradient vectors.

where $\mathbb{K}^M_{C^0}$ is the set

$$\mathbb{K}^M_{C^0} = \{\boldsymbol{U} \in \mathbb{R}^{2N} / \boldsymbol{A}\boldsymbol{U} \geq 0\}. \tag{35}$$

Like the previous problem (24), problem (34) is a standard linear finite-dimensional minimization problem since $\mathcal{P}(\boldsymbol{U})$ is a linear functional of the $2N$ parameters of nodal displacements collected in $\boldsymbol{U}$ whilst all the constraints (35) are represented by linear inequalities.

4. The church of "Pietà dei Turchini"

The two proposed numerical methods, that is PRD and C^0 methods, are now applied to a real case, namely the church of "Santa Maria Incoronatella della Pietà dei Turchini", an XVII century building located in Via Medina in Naples. During its life, a diffuse crack pattern due to foundation displacements interested this church. The fractures, detected before the recent restoration works, are depicted in Figure 3. This crack pattern was essentially the effect of a piecewise rigid body mechanism through which the masonry structure responded to the ground displacements.

The main aim is to use both methods for finding the foundation displacements producing the observed crack pattern. This case study was already analysed in [Iannuzzo et al. 2018a] by using the PRD method, but here a developed version has been used.

A second aim of present paper, beyond testing this developed version of PRD method, is to simulate the same problem with the C^0 method to compare these two numerical approximations and to find if and

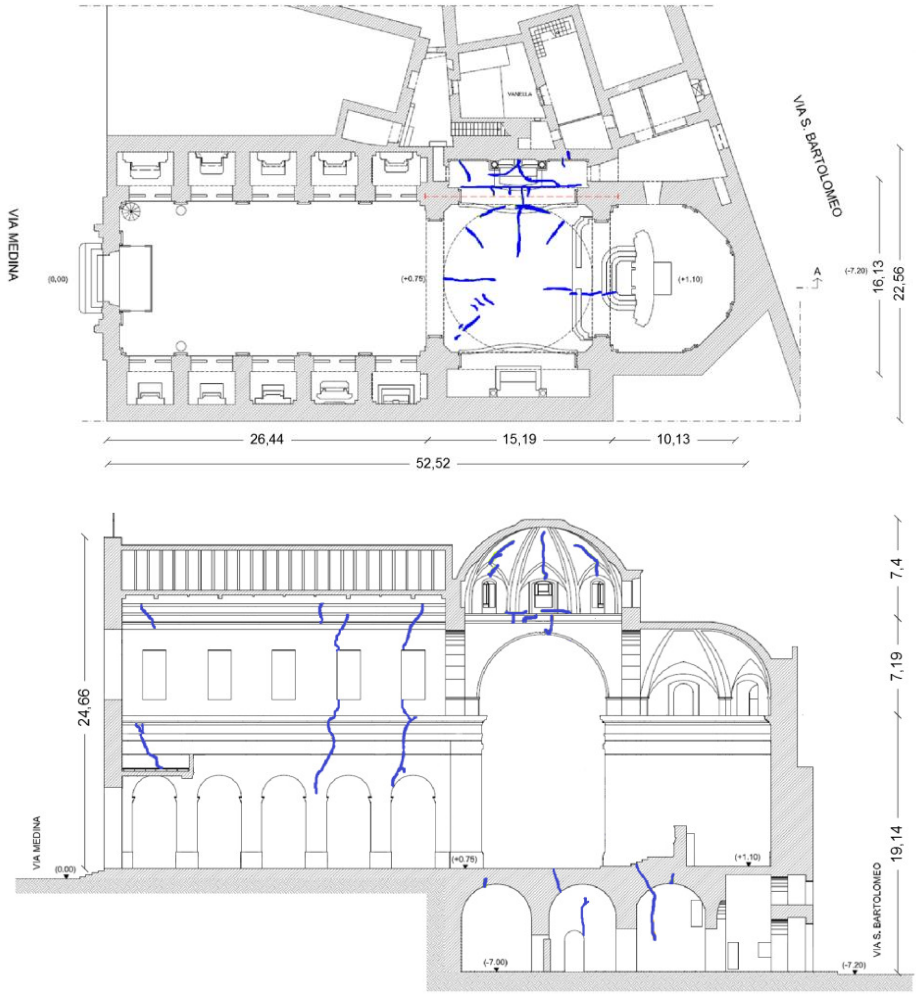

Figure 3. Plan (top) and section A-A′ (bottom) of the church showing the crack pattern.

how is possible to relate this two methods to get information about the best discretization that one can choose with the PRD method.

It is to be pointed out that though the crack pattern was fully manifested and consistent, the size of the rigid body movements produced by the given settlements remained everywhere small with respect to the overall size of the structure. Therefore, we can consider that the equilibrium state of the structure is not sensibly affected by these displacements, and a linearized kinematic analysis can be adopted.

The problem studied concerns the left wall of the central nave including the big arch of the transept and the left lateral wall of the apse (see Figure 3, bottom), treated as a plane case. The external loads acting on the structure are the mass density ($\rho = 1800\,\mathrm{kg/m^3}$) and uniformly distributed tractions, applied along external and internal lines, and representing the load exerted by secondary structures (see Figure 4).

In what follows the plane wall reported in Figure 4 is analysed by using both PRD and C^0 methods. Preliminarily the analysis is conducted by applying the PRD method and after some iterations, the

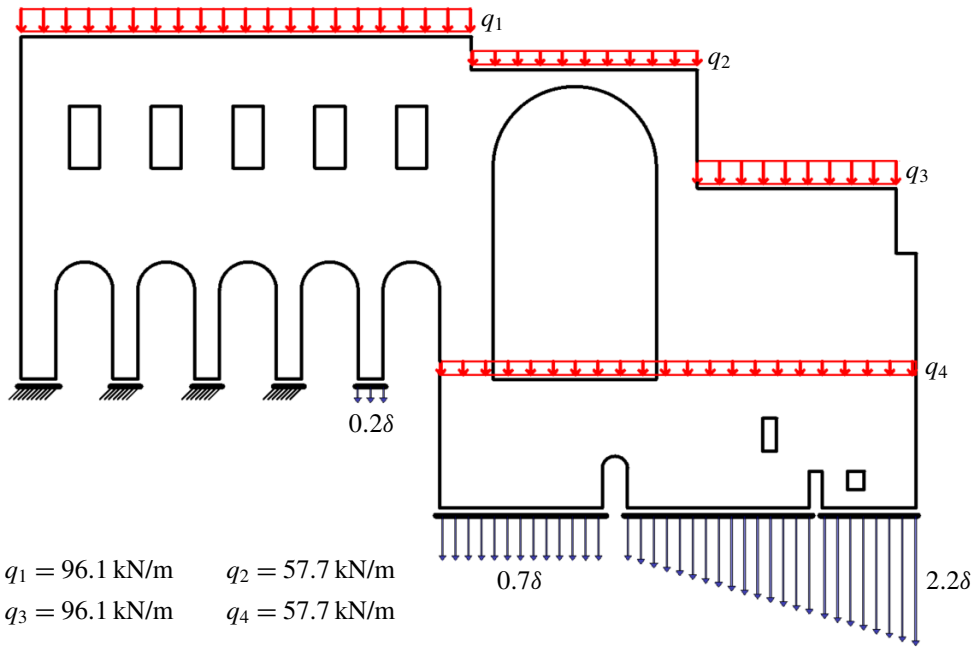

Figure 4. Structural scheme of the left wall of the central nave of the church. Distributed tractions due to the secondary structures and their values. Profile of the foundation displacements.

optimal profile of foundation displacements (depicted in Figure 4) has been found. In both cases the profile of foundation displacements has been used as boundary condition. The two numerical methods, implemented in Mathematica®, consist of the following main steps:

(1) definition of the structural geometry and of its discretization;

(2) characterization of the displacement field with support in the given discretization;

(3) characterization of the potential energy as a linear functional of the displacement parameters;

(4) definition of the internal and external constraints;

(5) numerical solution of the problem with a linear programming routine;

(6) postprocessing (evaluation of the displacement and strains corresponding to the solution).

4.1. ***Analysis through the PRD method.*** In Figure 5 the discretization adopted to implement the PRD method is shown. This real case was already analysed with the PRD method in [Iannuzzo et al. 2018a]. In this reference the structural scheme was discretized by using quadrilateral elements having only potential horizontal and vertical crack lines. In the present work, we redo the analysis by adopting a much richer mesh. Particularly, the discretization has been refined by adopting different kinds of polygonal rigid elements: starting from triangular elements going to hexagonal elements. Then, the discretization has been further cut by using diagonal lines in order to allow many potential diagonal cracks but at the same time without making any preferential choice.

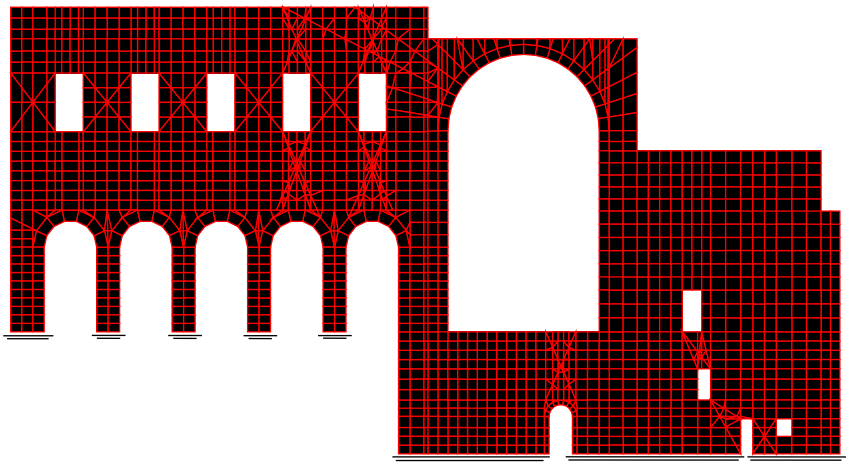

Figure 5. The rigid block discretization used with the PRD method: 2301 rigid polygonal elements are used.

The analysis is performed on a mesh of 2301 (rigid) polygonal elements (see Figure 5) and by considering the effect of the self-weight and of the external line loads shown in Figure 4. The total number of interfaces is 4650, of which 4068 are internal while the remaining 582 are external. Homogeneous conditions (16) and (17) have to be written for each internal interface, whilst boundary conditions, expressing the foundation settlements, have to be written at all external constrained interfaces.

The total number of unknowns is 6903; the number of restrictions (equalities and inequalities) is 16465. The solution of the minimum problem (24) was obtained with the interior point method in 57 s (with an Intel® Core™ i7-6700HQ) and, shown graphically in Figure 6.

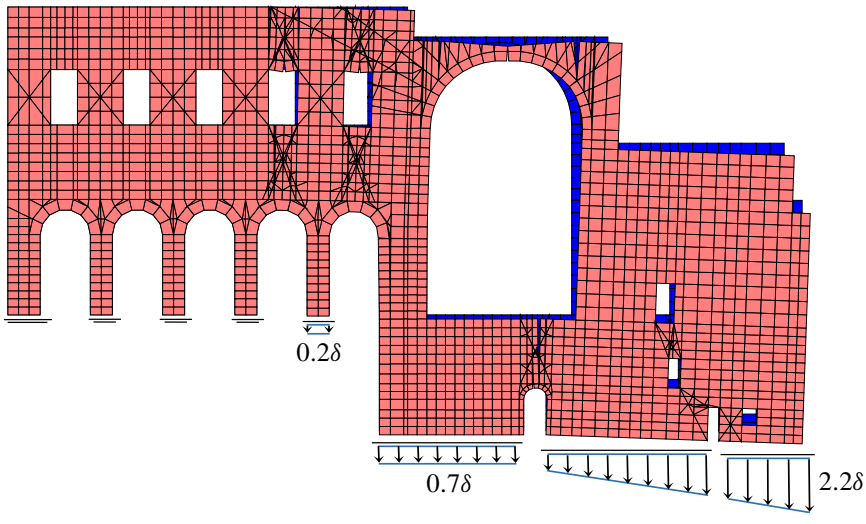

Figure 6. Displacement of the blocks corresponding to the solution of the minimum problem (11) obtained with the PRD method.

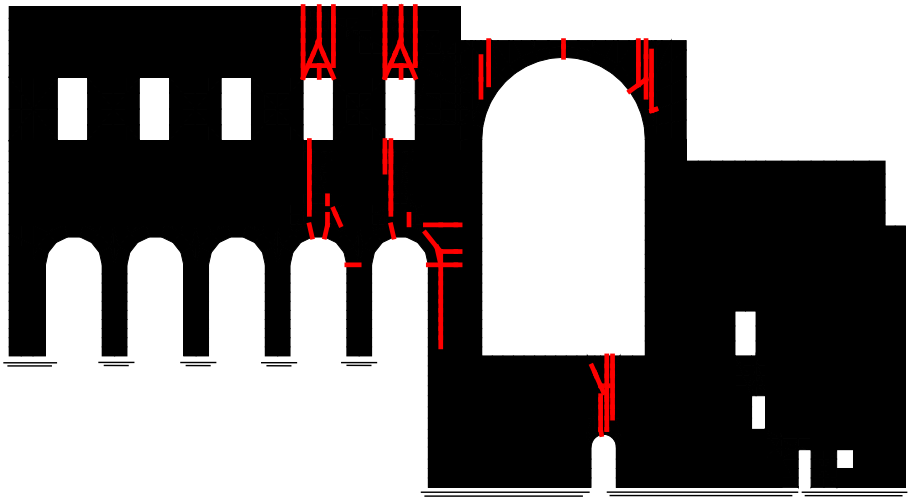

Figure 7. The internal interfaces on which there is a jump displacement are depicted with a red thick line.

In Figure 7 the internal interfaces on which there is a nonzero jump of the displacement field (that is the absolute values of the jump above a numerical threshold $10^{-2}\delta$) are underlined with a red thick line. The collection of such red lines gives a rough picture of the fracture pattern. The phenomenological observation that masonry structures, when subjected to settlements, exhibit a rigid macroblock mechanism, is perfectly caught by the numerical solution produced by the PRD method: the cracks (displacement jumps) concentrate on a selected set of a small number of interfaces and a *rigid macroblock partition* of the structural domain form.

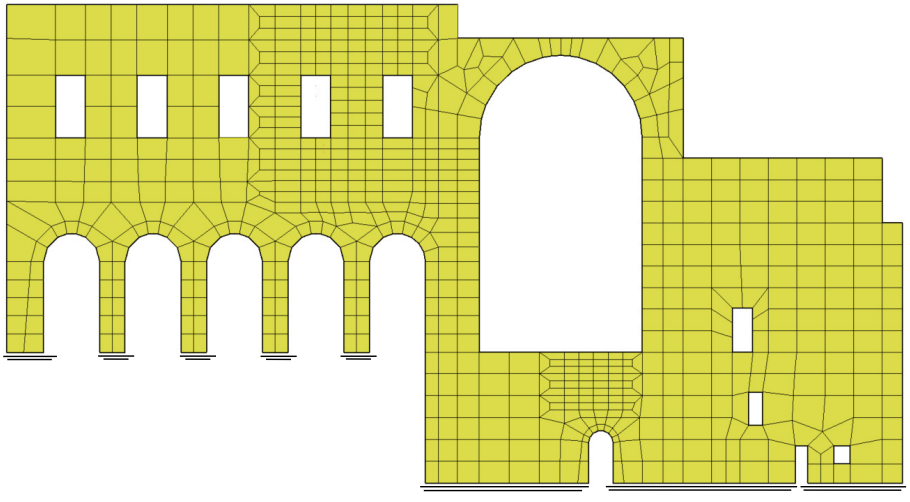

Figure 8. Plane section of Figure 3 (bottom) is here discretized into 677 square second-order Lagrangian elements.

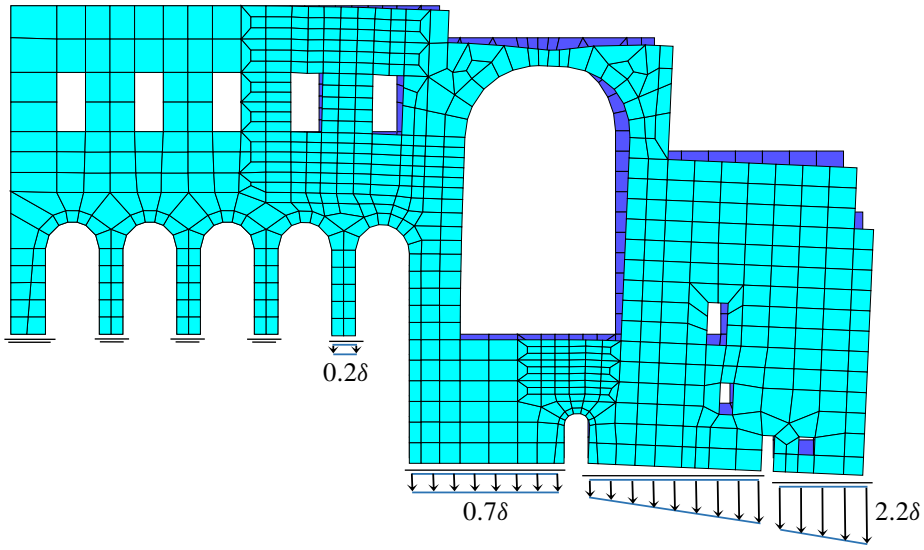

Figure 9. Displacement corresponding to the solution of the minimum problem (11) obtained with the C^0 method.

4.2. ***Analysis through the*** $\mathbf{C^0}$ ***method.*** The lateral section of Figure 3 (bottom) is here analysed with the C^0 method. The structure composed of NRNT material is discretized into 677 nine-node square elements (see [Bathe and Wilson 1976]). The external loads reported in Figure 4 and the self-weight applied at the centroid of each quadrilateral elements are considered.

The solution of the minimum problem (34), obtained with the interior point method in 300 s (with an Intel® Core™ i7-6700HQ) is shown graphically in Figure 9.

In this case, since the strain is purely regular (no singular strains are allowed), the strain is smeared and an indication of possible fractures is associated with zones where the displacement exhibits large gradients. In order to highlight such regions, the strain associated to the solution of the minimum problem (34) is graphically represented. A map of the regions over which the measure of $\boldsymbol{E}$, namely $|\boldsymbol{E}|^2 = \operatorname{tr}(\boldsymbol{E}\boldsymbol{E}^T)$, is nonzero is reported in Figure 10. From Figure 11, where a contour plot of $|\boldsymbol{E}|^2$ by using 200 level lines is reported. It can be observed that such fractures tend to nucleate in the neighbourhood of some lines. The remaining part of the domain is almost undeformed being characterized by strains whose norm is close to zero.

5. Comparison between PRD and $\mathbf{C^0}$ methods

The safety assessment of masonry structures interested by a crack pattern and then, the understanding of causes producing these effects, is one of the key issues in practical applications to real constructions. Several times, if we are not facing problems due to horizontal actions, the causes are represented by foundation displacements. However, these displacements cannot affect the stability of a structure and, therefore, they cannot drive the structure to the collapse as long as they are “small” in a certain sense. In fact, accommodating small changes of the external environment (in this case the kinematical data that is the foundation displacements) through a stable rigid macroblock partition of the structural domain is the

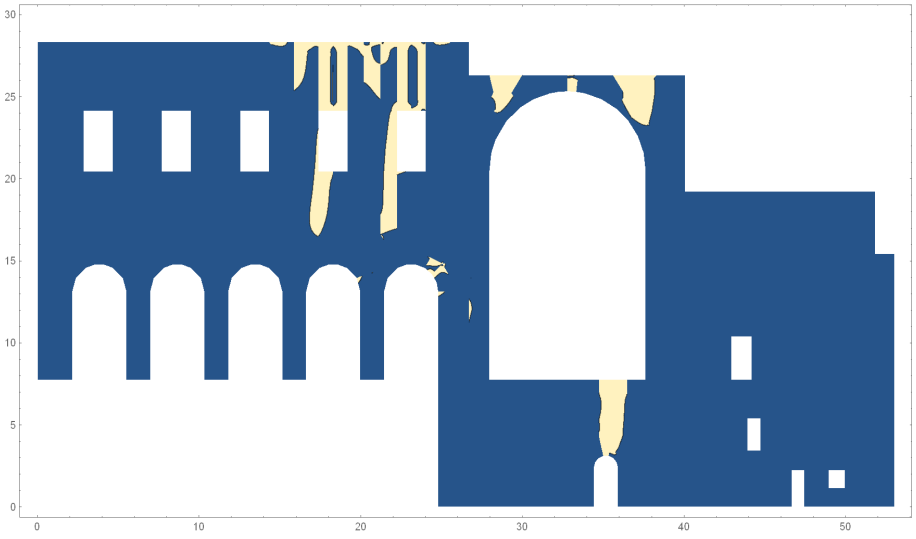

Figure 10. A map of the areas on which the norm of the strain $\boldsymbol{E}$, namely $|\boldsymbol{E}|^2 = \mathrm{tr}(\boldsymbol{E}\boldsymbol{E}^T)$, is greater than zero is reported: the remaining part of the domain, i.e., blue areas, is characterized by strains whose norm is close to zero.

peculiar behaviour of a masonry structure. Nevertheless, if the foundation displacements can increase, assessing if the structure is still stable in a new configuration and then evaluate its displacement capacity is the consequent concern. Anyway, behind both these two issues, there is, in a certain way, the same question: how to detect the rigid macroblock partition exhibited by a structure when it is subjected

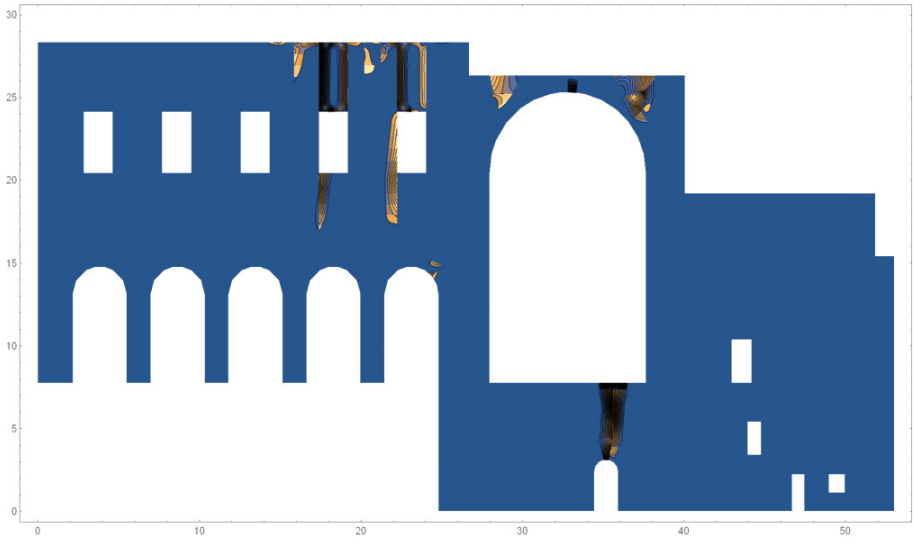

Figure 11. Contour plot of the strain field by using 200 contour level lines: fractures are concentrated along certain lines.

to foundation displacements? Because of the intrinsic unilateral behaviour of a masonry structure, the answer is not trivial and, so far, no computational tools, at least for generic structures, has been developed for this aim.

To tackle this problem, and then for setting up a numerical model able to detect the rigid macroblock nucleation, it is reasonable to work with small displacements since the goal is to define a partition on the initial configuration. If the size of the displacements is small related to the overall size of the structure, the error made in considering small displacements rather than finite ones is small and, one can also relate the size of the openings (cracks) to the foundation displacements.

Both the methods here presented, PRD and C^0 methods, have been developed to answer this question and are based on the small displacements assumption that also allows to make the optimization problem linear and then to solve it in a few seconds. As a consequence of this fast calculation speed, particularly for the PRD method, these are suitable tools for solving an inverse problem, since many trials in an iterative procedure have to be performed for individuating the optimal profile of foundation displacements giving the best qualitative fit with the actual crack pattern. In the case of small settlements, as stated before, a reasonable estimation of their size can be achieved by relating them with the width of the cracks.

One of the main issues addressed in this paper was the definition of the partition adopted with the PRD method. In fact, it is intuitively clear that the solution obtained with the PRD method depends on the initial partition much more than the one got with C^0 method. For instance, in [Iannuzzo et al. 2018a] it has been shown a shortcoming of the PRD method: the solution cannot converge to a concentrated crack whose support is not parallel to the skeleton of the mesh, that is, jump discontinuities along zigzag lines are not kinematically admissible. The C^0 method does not suffer from this defect, and though more cumbersome from the numerical point of view, can converge to cracks whose support is not parallel to the interfaces of the elements.

On the contrary, as shown with many benchmark cases in [Iannuzzo et al. 2018a], if an "optimal" discretization of the domain is suggested by the stereotomy of the real structure (e.g., arched structures), the results of the PRD method are impressive when compared to analytical ones.

However, in this case study no information about an opportune discretization into rigid blocks is available, and the partition adopted with both methods has been driven by the detected crack pattern in the sense that, as one can see from figures 5 and 9, the mesh is much more refined on areas interested by the cracks. Whilst for the C^0 method (see Figure 9) this was done only for reducing the computational time, for the PRD method the need of taking into account also diagonal cracks was the main concern. In fact, by looking at Figure 5 it is possible to see that many potential crack lines have been added in areas where the mesh has been refined, but without doing any preferential choice on them.

In Figure 12, the overlap of the solutions got with the two methods is reported and a perfect concordance of the displacements obtained with the two methods can be observed.

In Figure 13 the concentrated cracks obtained with the PRD method and the smeared cracks obtained with the C^0 method are compared. From this figure, again a good concordance between fractures obtained with these two methods is detected. Furthermore, the solution got with C^0 method, even if it is based on continuous functions, concentrates smeared cracks in small areas returning an approximate partition of the whole structure into rigid blocks, confirming the validity of the PRD approach.

In this respect, it is to point out that the appearance of piecewise rigid mechanisms (producing concentrated strains) rather than continuous mechanisms (entailing diffuse strains), is often due, in real

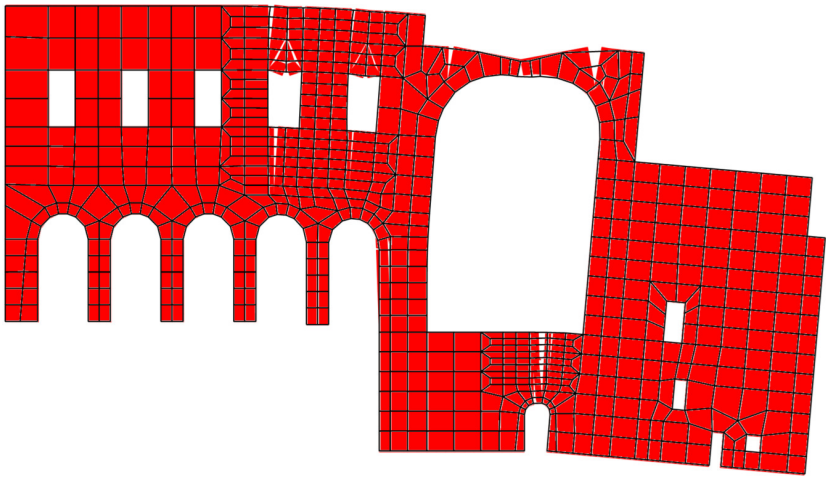

Figure 12. Overlapping of the solutions obtained with the two methods: in the background in red the solution with the PRD method is represented, whilst the black skeleton mesh represents the solution reached with the C^0 method.

structures, to mechanical characteristics, such as cohesion, toughness and finite friction, which are not accounted by the NRNT model.

This perfect concordance among the solutions in terms of both displacements and fractures, gives a hint about a further potential use of C^0 method: if no information on the discretization for PRD method can be obtained from the actual stereotomy, beyond using a clever partition where any kind of potential crack lines are allowed, the C^0 method could be used for selecting the rigid macroblock discretization to be fed into the PRD method.

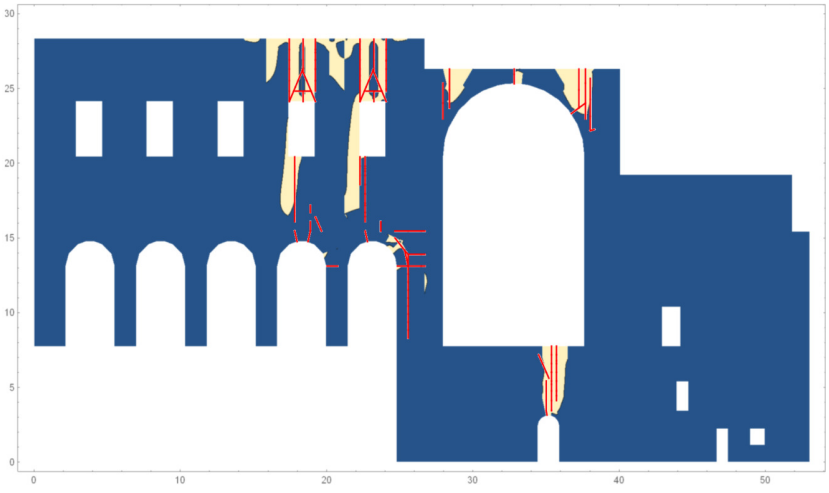

Figure 13. Overlapping of the solutions obtained with the two methods: in red the solution obtained in terms of cracks with the PRD method and in white the zones of smeared cracks.

6. Conclusions

In practical applications to real structures, one of the main issues is to identify the optimal profile of foundation displacements, that is, the settlements giving the best qualitative fit with the detected crack pattern. With this in mind, a study concerning the "Chiesa di Santa Maria Incoronatella della Pietà dei Turchini" is here proposed. The church is modelled as composed by NRNT material and two numerical methods, that is PRD and C^0 methods, are applied. With both the methods the solution of the BVP is represented by the minimizer of the potential energy of the loads, and it is obtained by discretizing the problem in two different suitable functional spaces: with the PRD method the energy is minimized within the set of piecewise rigid displacements whilst with the C^0 method the search of the minimum is restricted to continuous displacement fields.

By using small displacements, the optimization problem becomes linear and can be solved with standard algorithms used for linear programming optimization, such as interior-point method (here adopted) allowing to reach solutions in a few seconds.

The optimal profile of foundation displacements was found with the PRD method in an iterative procedure. The detected crack pattern drove the discretization, in the sense that the partition is much more refined in those areas where the cracks were observed and it is further cut by diagonal lines for reproducing other potential crack lines. This is due to a shortcoming of the PRD method: when the stereotomy of the structure does not suggest any particular partition (e.g., for arched structures), the best way to tackle the problem is to allow cleverly many kinds of potential crack lines but avoiding any a priori choice.

Once the optimal profile of foundation displacements was found through the PRD method, the C^0 has been applied by using this profile as boundary condition. The results in terms of displacements and fractures show an impressive concordance among these two different numerical approximations. In particular, the main result of the C^0 method is that, even if continuous functions are considered, the solution returns an approximate partition of the whole structure into rigid blocks, confirming the validity of the PR method approach.

Furthermore, these results suggest that the C^0 method, being more time consuming, is more appropriate in the analysis of simple structures or as a preliminary tool for defining the rigid macroblock partition to be implemented in the PRD method.

References

[Addessi and Sacco 2018] D. Addessi and E. Sacco, "Homogenization of heterogeneous masonry beams", *Meccanica* (*Milano*) **53**:7 (2018), 1699–1717.

[Angelillo 1993] M. Angelillo, "Constitutive relations for no-tension materials", *Meccanica* (*Milano*) **28**:3 (1993), 195–202.

[Angelillo 2014] M. Angelillo, "Practical applications of unilateral models to masonry equilibrium", pp. 109–210 in *Mechanics of masonry structures*, edited by M. Angelillo, Springer, Vienna, 2014.

[Angelillo 2019] M. Angelillo, "The model of Heyman and the statical and kinematical problems for masonry structures", *Int. J. Masonry Res. Innov.* **4**:1-2 (2019), 14–31.

[Angelillo and Fortunato 2004] M. Angelillo and A. Fortunato, "Equilibrium of masonry vaults", pp. 105–111 in *Novel approaches in civil engineering*, edited by M. Frémond and F. Maceri, Springer, Berlin, Heidelberg, 2004.

[Angelillo and Rosso 1995] M. Angelillo and F. Rosso, "On statically admissible stress fields for a plane masonry-like structure", *Quart. Appl. Math.* **53**:4 (1995), 731–751.

[Angelillo et al. 2010] M. Angelillo, L. Cardamone, and A. Fortunato, "A numerical model for masonry-like structures", *J. Mech. Mater. Struct.* **5**:4 (2010), 583–615.

[Angelillo et al. 2012] M. Angelillo, E. Babilio, and A. Fortunato, "Numerical solutions for crack growth based on the variational theory of fracture", *Comput. Mech.* **50**:3 (2012), 285–301.

[Angelillo et al. 2014] M. Angelillo, A. Fortunato, A. Montanino, and M. Lippiello, "Singular stress fields in masonry structures: Derand was right", *Meccanica* (*Milano*) **49**:5 (2014), 1243–1262.

[Angelillo et al. 2016] M. Angelillo, E. Babilio, A. Fortunato, M. Lippiello, and A. Montanino, "Analytic solutions for the stress field in static sandpiles", *Mech. Mater.* **95** (2016), 192–203.

[Angelillo et al. 2018] M. Angelillo, A. Fortunato, A. Gesualdo, A. Iannuzzo, and G. Zuccaro, "Rigid block models for masonry structures", *Int. J. Masonry Res. Innov.* **3**:4 (2018), 349–368.

[Bagi 2014] K. Bagi, "When Heyman's Safe Theorem of rigid block systems fails: non-Heymanian collapse modes of masonry structures", *Int. J. Solids Struct.* **51**:14 (2014), 2696–2705.

[Bathe and Wilson 1976] K.-J. Bathe and E. L. Wilson, *Numerical methods in finite element analysis*, Prentice-Hall, 1976.

[Block 2009] P. Block, *Thrust network analysis: exploring three-dimensional equilibrium*, Ph. D. thesis, Massachusetts Institute of Technology. Dept. of Architecture., 2009, Available at https://dspace.mit.edu/handle/1721.1/49539.

[Block and Lachauer 2013] P. Block and L. Lachauer, "Three-dimensional (3D) equilibrium analysis of gothic masonry vaults", *Int. J. Archit. Herit.* **8**:3 (2013), 312–335.

[Block and Lachauer 2014] P. Block and L. Lachauer, "Three-dimensional funicular analysis of masonry vaults", *Mech. Res. Commun.* **56** (2014), 53–60.

[Block et al. 2006] P. Block, M. De Jong, and J. Ochsendorf, "As hangs the flexible line: equilibrium of masonry arches", *Nexus Netw. J.* **8**:2 (2006), 13–24.

[Brandonisio et al. 2015] G. Brandonisio, E. Mele, and A. De Luca, "Closed form solution for predicting the horizontal capacity of masonry portal frames through limit analysis and comparison with experimental test results", *Eng. Fail. Anal.* **55** (2015), 246–270.

[Brandonisio et al. 2017] G. Brandonisio, E. Mele, and A. De Luca, "Limit analysis of masonry circular buttressed arches under horizontal loads", *Meccanica* (*Milano*) **52**:11-12 (2017), 2547–2565.

[Castellano 1988] G. Castellano, "Un modello cinematico per i materiali non resistenti a trazione", in *Cinquantenario della Facoltà di Architettura di Napoli: Franco Jossa e la sua opera*, Napoli, 1988.

[Cennamo et al. 2018] C. Cennamo, C. Cusano, A. Fortunato, and M. Angelillo, "A study on form and seismic vulnerability of the dome of San Francesco di Paola in Naples", *Ing. Sismica* **35**:1 (2018), 88–108.

[Chambolle et al. 2007] A. Chambolle, A. Giacomini, and M. Ponsiglione, "Piecewise rigidity", *J. Funct. Anal.* **244**:1 (2007), 134–153.

[Como 1992] M. Como, "Equilibrium and collapse analysis of masonry bodies", *Meccanica* (*Milano*) **27**:3 (1992), 185–194.

[Coulomb 1776] C. A. Coulomb, "Essai sur une application des règles de maximis & minimis à quelques problèmes de statique: relatifs à l'architecture", *Mémoires de mathématique & de physique, présentés à l'Académie Royale des Sciences par divers savans* **7** (1776), 343–382.

[Couplet 1729] P. Couplet, "De la poussée des voûtes", *Mémoires de l'Académie Royale des Sciences* (1729), 79–117.

[Couplet 1730] P. Couplet, "Seconde partie de l'examen de la poussée des voûtes", *Mémoires de l'Académie Royale des Sciences* (1730), 117–141.

[Dantzig 1963] G. Dantzig, *Linear programming and extensions*, Princeton university press, 1963.

[Danyzy 1732/1778] A. A. H. Danyzy, "Méthode générale pour déterminer la résistance qu'il faut opposer à la poussée des voûtes", *Histoire de la Société Royale des Sciences établie à Montpellier* **2**:1718-1745 (1732/1778), 40–56.

[De Serio et al. 2018] F. De Serio, M. Angelillo, A. Gesualdo, A. Iannuzzo, G. Zuccaro, and M. Pasquino, "Masonry structures made of monolithic blocks with an application to spiral stairs", *Meccanica* (*Milano*) **53**:8 (2018), 2171–2191.

[Del Piero 1998] G. Del Piero, "Limit analysis and no-tension materials", *Int. J. Plast.* **14**:1-3 (1998), 259–271.

[Di Pasquale 1984] S. Di Pasquale, *Statica dei solidi murari: teoria ed esperienze*, Università di Firenze: Atti Dipartimento Costruzioni, 1984.

[Fortunato et al. 2014] A. Fortunato, F. Fraternali, and M. Angelillo, "Structural capacity of masonry walls under horizontal loads", *Ing. Sismica* **31**:1 (2014), 41–49.

[Fortunato et al. 2016] A. Fortunato, E. Babilio, M. Lippiello, A. Gesualdo, and M. Angelillo, "Limit analysis for unilateral masonry-like structures", *Open Construct. Build. Technol. J.* **10**:Suppl 2: M12 (2016), 346–362.

[Fortunato et al. 2018] A. Fortunato, F. Fabbrocino, M. Angelillo, and F. Fraternali, "Limit analysis of masonry structures with free discontinuities", *Meccanica* (*Milano*) **53**:7 (2018), 1793–1802.

[Fraddosio et al. 2019] A. Fraddosio, N. Lepore, and M. D. Piccioni, "Lower bound limit analysis of masonry vaults under general load conditions", pp. 1090–1098 in *Structural analysis of historical constructions*, edited by R. Aguilar et al., Springer, Cham, 2019.

[Gesualdo and Monaco 2015] A. Gesualdo and M. Monaco, "Constitutive behaviour of quasi-brittle materials with anisotropic friction", *Lat. Am. J. Solids Struct.* **12**:4 (2015), 695–710.

[Gesualdo et al. 2017] A. Gesualdo, C. Cennamo, A. Fortunato, G. Frunzio, M. Monaco, and M. Angelillo, "Equilibrium formulation of masonry helical stairs", *Meccanica* (*Milano*) **52**:8 (2017), 1963–1974.

[Gesualdo et al. 2018] A. Gesualdo, A. Iannuzzo, M. Monaco, and F. Penta, "Rocking of a rigid block freestanding on a flat pedestal", *J. Zhejiang Univ. Sci. A* **19**:5 (2018), 3310–345.

[Giaquinta and Giusti 1985] M. Giaquinta and E. Giusti, "Researches on the equilibrium of masonry structures", *Arch. Ration. Mech. Anal.* **88**:4 (1985), 359–392.

[Giuffrè 1991] A. Giuffrè, *Letture sulla Meccanica delle Murature Storiche*, Edizioni Kappa, 1991.

[Gregory 1695] D. Gregory, "Catenaria", *Philos. Trans. Royal Soc.* **19**:231 (1695), 637–652.

[Heyman 1966] J. Heyman, "The stone skeleton", *Int. J. Solids Struct.* **2**:2 (1966), 249–279.

[Heyman 1998] J. Heyman, *Structural analysis: a historical approach*, Cambridge University Press, Cambridge, 1998.

[Hooke 1676] R. Hooke, *A description of helioscopes and some other instruments made by Robert Hooke, fellow of the Royal Society*, T.R. for John Martyn, London, 1676.

[Huerta 2006] S. Huerta, "Galileo was wrong: the geometrical design of masonry arches", *Nexus Netw. J.* **8**:2 (2006), 25–52.

[Huerta 2008] S. Huerta, "The analysis of masonry architecture: a historical approach: to the memory of professor Henry J. Cowan", *Architect. Sci. Rev.* **51**:4 (2008), 297–328.

[Iannuzzo 2017] A. Iannuzzo, *A new rigid block model for masonry structures*, Ph. D. dissertation, Department of Structures for Engineering and Architecture, Università degli Studi di Napoli Federico II, 2017, Available at http://www.fedoa.unina.it/11732/1/Iannuzzo_Antonino_29.pdf.

[Iannuzzo et al. 2018a] A. Iannuzzo, M. Angelillo, E. De Chiara, F. De Guglielmo, F. De Serio, F. Ribera, and A. Gesualdo, "Modelling the cracks produced by settlements in masonry structures", *Meccanica* (*Milano*) **53**:7 (2018), 1857–1873.

[Iannuzzo et al. 2018b] A. Iannuzzo, A. De Luca, A. Fortunato, A. Gesualdo, and M. Angelillo, "Fractures detection in masonry constructions under horizontal seismic forces", *Ing. Sismica* **35**:3 (2018), 87–103.

[Iannuzzo et al. 2018c] A. Iannuzzo, F. De Serio, A. Gesualdo, G. Zuccaro, A. Fortunato, and M. Angelillo, "Crack patterns identification in masonry structures with a C° displacement energy method", *Int. J. Masonry Res. Innov.* **3**:3 (2018), 295–323.

[Kooharian 1952] A. Kooharian, "Limit analysis of voussoir (segmental) and concrete arches", *J. Am. Concrete Ins.* **49**:24 (1952), 317–328.

[Kurrer 2008] K.-E. Kurrer, "The history of the theory of structures: from arch analysis to computational mechanics", *Int. J. Space Struct.* **23**:3 (2008), 193–197.

[Le Seur et al. 1742] T. Le Seur, F. Jacquier, and R. G. Boscovich, *Parere di tre mattematici sopra i danni che si sono trovati nella cupola di S. Pietro sul fine dell'anno 1742*, Roma, 1742.

[Livesley 1978] R. K. Livesley, "Limit analysis of structures formed from rigid blocks", *Int. J. Numer. Methods Eng.* **12**:12 (1978), 1853–1871.

[Marmo and Rosati 2017] F. Marmo and L. Rosati, "Reformulation and extension of the thrust network analysis", *Comput. Struct.* **182** (2017), 104–118.

[Marmo et al. 2018] F. Marmo, D. Masi, and L. Rosati, "Thrust network analysis of masonry helical staircases", *Int. J. Archit. Herit.* **12**:5 (2018), 828–848.

[Mehrotra 1992] S. Mehrotra, "On the implementation of a primal-dual interior point method", *SIAM J. Optim.* **2**:4 (1992), 575–601.

[Milani 2011] G. Milani, "Simple lower bound limit analysis homogenization model for in- and out-of-plane loaded masonry walls", *Constr. Build. Mater.* **25**:12 (2011), 4426–4443.

[Monaco et al. 2014] M. Monaco, M. Guadagnuolo, and A. Gesualdo, "The role of friction in the seismic risk mitigation of freestanding art objects", *Nat. Hazards* **73**:2 (2014), 389–402.

[Ochsendorf 2006] J. Ochsendorf, "The masonry arch on spreading supports", *Struct. Eng.* **84**:2 (2006), 29–34.

[Poleni 1748] G. Poleni, *Memorie istoriche della gran cupola del tempio Vaticano e de'danni di essa e detristoramenti loro, divisi in libri cinque*, Nella stamperia del seminario, Padova, 1748.

[Portioli et al. 2014] F. Portioli, C. Casapulla, M. Gilbert, and L. Cascini, "Limit analysis of 3D masonry block structures with non-associative frictional joints using cone programming", *Comput. Struct.* **143** (2014), 108–121.

[Romano and Romano 1979] G. Romano and M. Romano, "Sulla soluzione di problemi strutturali in presenza di legami costitutivi unilaterali", *Atti della Accademia Nazionale dei Lincei. Classe di Scienze Fisiche, Matematiche e Naturali. Rendiconti* **67**:1-2 (1979), 104–113.

[Sacco 2014] E. Sacco, "Micro, multiscale and macro models for masonry structures", pp. 241–291 in *Mechanics of masonry structures*, edited by M. Angelillo, Springer, Vienna, 2014.

[Shin et al. 2016] H. V. Shin, C. F. Porst, E. Vouga, J. Ochsendorf, and F. Durand, "Reconciling elastic and equilibrium methods for static analysis", *ACM Trans. Graph.* **35**:2 (2016), article 13.

[Van Mele et al. 2012] T. Van Mele, J. McInerney, M. DeJong, and P. Block, "Physical and computational discrete modeling of masonry vault collapse", pp. 2252–2560 in *Proceedings of the 8th International Conference on Structural Analysis of Historical Constructions Wroclaw* (Wroclaw, Poland), 2012.

[Šilhavý 2014] M. Šilhavý, "Mathematics of the masonry-like model and limit analysis", pp. 29–69 in *Mechanics of masonry structures*, edited by M. Angelillo, Springer, Vienna, 2014.

[Yvon Villarceau 1853] A. Yvon Villarceau, *Sur l'établissement des arches de pont, envisagé au point de vue de la plus grande stabilité: mémoire accompagné de tables pour faciliter les applications numériques*, Imprimerie impériale, 1853.

[Yvon Villarceau 1854] A. Yvon Villarceau, *L'établissement des arches de pont*, Institut de France, Académie des Sciences, 1854.

[Zuccaro et al. 2017] G. Zuccaro, F. Dato, F. Cacace, D. De Gregorio, and S. Sessa, "Seismic collapse mechanisms analyses and masonry structures typologies: a possible correlation", *Ing. Sismica* **34**:4 (2017), 121–149.

Received 14 Dec 2018. Revised 9 Sep 2019. Accepted 28 Sep 2019.

ANTONINO IANNUZZO: iannuzzo@arch.ethz.ch
Institute of Technology in Architecture, Block Research Group, ETH Zurich, Stefano-Franscini-Platz 1, 8093 Zurich, Switzerland

JOURNAL OF MECHANICS OF MATERIALS AND STRUCTURES

msp.org/jomms

Founded by Charles R. Steele and Marie-Louise Steele

Cover photo: Mando Gomez, www.mandolux.com

See msp.org/jomms for submission guidelines.

JoMMS (ISSN 1559-3959) at Mathematical Sciences Publishers, 798 Evans Hall #6840, c/o University of California, Berkeley, CA 94720-3840, is published in 10 issues a year. The subscription price for 2019 is US $635/year for the electronic version, and $795/year (+$60, if shipping outside the US) for print and electronic. Subscriptions, requests for back issues, and changes of address should be sent to MSP.

JoMMS peer-review and production is managed by EditFLOW® from Mathematical Sciences Publishers.

PUBLISHED BY

mathematical sciences publishers

nonprofit scientific publishing

http://msp.org/

Journal of Mechanics of Materials and Structures

Volume 14, No. 5 December 2019

1559-3959(2019)14:5;1-T